ORGANIC CHEMISTRY

Stereoretentive radical-based alkyl-alkyl cross-coupling

Yu Wang[1]†, Jiawei Sun[1]†, Yin Li[1]†, David A. Cagan[1]†, Oliver T. Ring[1], Xin Zeng[1], Jet Tsien[1], Luca Massaro[1], Jillian E. Smith[2], Brandon J. Orzolek[2], Michael R. Collins[3], Yu Kawamata[1], Phil S. Baran[1]*

The construction of stereogenic C(sp^3)–C(sp^3) bonds through cross-coupling remains a formidable challenge owing to competing β-hydride elimination and homocoupling as well as the poor inherent stereocontrol of radical pathways. In this work, we report a scalable stereoretentive radical-radical cross-coupling of two distinct, transient alkyl radicals, derived from enantioenriched sulfonylhydrazides and achiral primary and secondary alkyl halides, achieved without chiral ligands, directing groups, or exogenous redox agents. This substrate-controlled approach leverages a nickel-catalyzed, redox-neutral manifold, which enables precise kinetic matching of diazene-mediated radical generation and halogen atom transfer. The reaction produced enantiospecificities of 80 to 96% and synthetically useful yields (up to 90%) across diverse piperidine and pyrrolidine scaffolds while tolerating ethers, free amines, aryl halides, heterocycles, olefins, and other sensitive motifs. Mechanistic studies support caged radical rebound at nickel to preserve chirality, followed by nickel(I)-nickel(III)–mediated radical capture and reductive elimination.

The construction of C(sp^3)–C(sp^3) bonds, particularly to produce stereogenic centers, stands as a cornerstone of modern organic synthesis, enabling access to the three-dimensional molecular architectures that underpin bioactive natural products, pharmaceuticals, and advanced materials (*1*–*4*). Although traditional cross-coupling paradigms have revolutionized C(sp^2)–C(sp^2) and C(sp^2)–C(sp^3) fragment assembly (*5*–*7*), their extension to C(sp^3)–C(sp^3) linkages has been stymied by persistent mechanistic hurdles, including β-hydride elimination, sluggish reductive elimination from dialkyl metal complexes, and poor cross-selectivity in radical-based protocols (Fig. 1A) (*8*). Radical-radical cross-coupling (RRCC) emerges as a compelling alternative, leveraging open-shell pathways to bypass these limitations and harness abundant feedstocks, such as carboxylic acids, amines, olefins, alcohols, and halides, for modular bond formation (*9*–*15*). Yet, achieving controlled RRCC without stereochemical bias remains daunting owing to fundamental reactivity constraints: Diffusion-controlled radical recombination often yields statistical mixtures of homodimers and cross-products, which necessitates persistent radical effects (radical precursors with adjacent stabilizing groups), radical-sorting catalysts, or excess stoichiometry to enforce selectivity (*16*–*26*). The pursuit of enantioselective RRCC amplifies these challenges substantially because transient alkyl radicals defy precise stereocontrol; to date, breakthroughs have relied on chiral ligands, auxiliaries, or dual-catalyst systems to template asymmetric induction, often at the cost of substrate generality and operational simplicity (*27*–*39*). If such a process could be achieved, it would change the way chemists synthesize chiral molecules. For instance, building block **1**, previously used in a medicinal chemistry campaign, was prepared in a seven-step process using polar bond analysis for which only a single skeletal bond was created (Horner–Wadsworth–Emmons reaction) and necessitating a chiral resolution (*40*). By contrast, a hypothetical stereoretentive RRCC would substantially simplify access to such structures. In this work, we disclose the realization of this goal with the stereospecific coupling of two distinct, transient carbon radicals, derived from a chiral sulfonylhydrazide and an achiral alkyl halide, without the aid of chiral catalysts. This substrate-controlled manifold delivers enantioenriched products with high fidelity, offering a paradigm shift in asymmetric RRCC by embedding stereochemical information directly into the radical precursor, thereby streamlining access to diversely functionalized chiral motifs from bench-stable building blocks.

Inspired by recent precedent in stereoretentive arylation through radical-polar coupling (*41*), wherein chiral sulfonylhydrazides **2** serve as effective radical surrogates to deliver enantioenriched products using an achiral nickel catalyst and aryl halides under mildly basic conditions in alcohol solvents, we hypothesized that this paradigm could be extended to achieve enantiospecific alkyl-alkyl RRCC (Fig. 1B). In that study, base liberates a diazene intermediate **4** from enantioenriched sulfonylhydrazide **2** that presumably reacts with a Ni(4-Clbpy)(Ar)X complex **5** through a cyclic transition state **6** that is driven to the arylated product **7** through N_2 evolution, thereby leading to high levels of stereoretention [up to 95% enantiospecificity (e.s.)]. Extending this precedent to the challenge of RRCC would require a precise kinetic matching (*42*) of events wherein a Ni catalyst would be involved in both base-mediated sulfonylhydrazide activation to stereoretentively form a chiral Ni–C intermediate **11** (after diazene **9** decomposition with loss of N_2 via a caged radical intermediate **10**) and halogen atom transfer (XAT) with an alkyl halide **8** to generate a transient alkyl radical **14**. The union of Ni complex **11** with **14** would then deliver an enantioenriched RRCC product **15**, thereby preserving the stereochemical integrity of the chiral alkyl fragment without requiring chiral ligands. Unlike radical cross-coupling (RCC) arylation, which uses a bidentate ligand, it was hypothesized that a tridentate ligand would be necessary to stabilize intermediate **11** (*43*–*45*). This approach would address the long-standing challenge of controlling radical-radical recombination by leveraging the specific reactivity of two different radical precursors: sulfonylhydrazides, which through in-cage diazene tethering retain chirality, and alkyl halides, which through rapid XAT deliver a transient free radical. Although the direct application of the protocol reported previously for stereoretentive arylative RCC provided an initial hit, it required an extensive overhaul with a completely new set of conditions (Fig. 2).

Reaction development

To arrive at the optimized conditions for stereoretentive RRCC, studies were initiated using an enantioenriched piperidine sulfonylhydrazide (n = 1, where n refers to the number of methylene units) bearing a Cbz protecting group and iodide **16** as a model system. Drawing from prior conditions for stereoretentive arylation (*41*) that used a Ni(4-Clbpy)$(NO_3)_2$ precatalyst (3 mol %) in *t*-amyl alcohol (0.2 M) at 40°C, the desired coupling product was afforded in only 6% yield and 38% enantiospecificity (Fig. 2, entry 1). Switching to a Ni precatalyst bearing a tridentate ligand **Ni-1** (the structure of this Ni complex was verified by x-ray crystallography) and using trifluoroethanol (TFE) as solvent improved the yield to 52% but maintained moderate e.s. at 56% (entry 2). Protecting group variations revealed that a Boc group yielded 35% product with 61% e.s. (entry 3), whereas Ts provided a lower 29% yield but higher 72% e.s. (entry 4). Notably, removing the protecting group entirely (free NH, R = H) further enhanced e.s. to 94%, albeit in a modest 14% yield (entry 5). The major by-product in this entry was piperidine along with unreacted **16**, which suggests that the hydrazide consumption was rapid, whereas activation of the alkyl iodide was slow; *N*-alkylation of the piperidine with the alkyl iodide was not observed in TFE. It was reasoned that because the unprotected piperidinyl sulfonylhydrazide (free NH, R = H) is a bis-HCl salt, additional base would be needed to fully reveal the

[1]Department of Chemistry, Scripps Research, La Jolla, CA, USA. [2]Automated Synthesis Facility, Scripps Research, La Jolla, CA, USA. [3]Department of Chemistry, La Jolla Laboratories, Pfizer Inc., San Diego, CA, USA. ***Corresponding author. Email: pbaran@scripps.edu** †These authors contributed equally to this work.

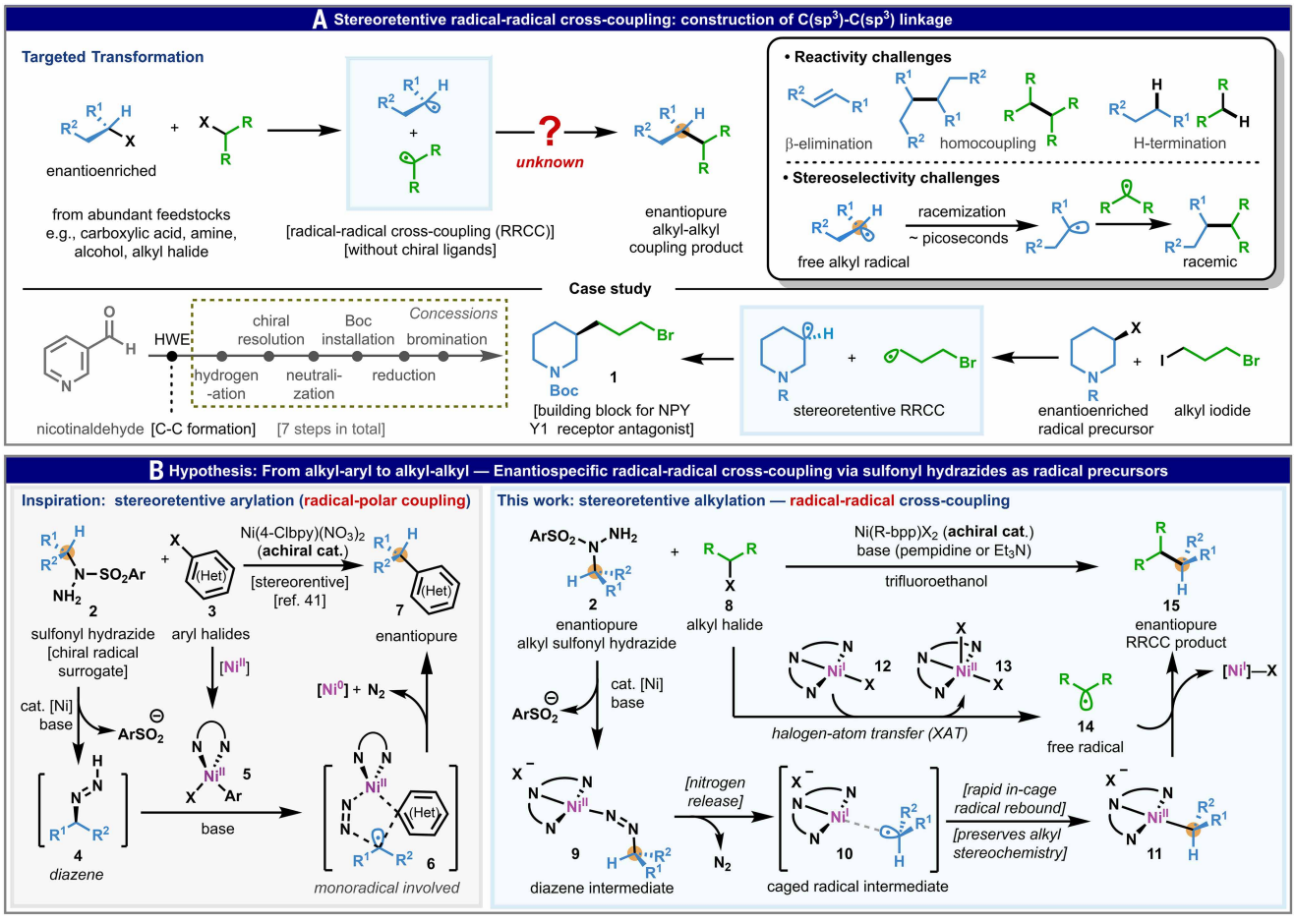

Fig. 1. Background and reaction conception. (**A**) Precedent and challenges of the targeted transformation, RRCC, with a case study of a potential RRCC application. (**B**) Hypothesis of stereoretentive RRCC of alkyl sulfonylhydrazides to make C(sp^3)–C(sp^3) bonds. Boc, *tert*-butoxycarbonyl.

hydrazide and aid in its coordination to Ni (*42*). Increasing the pempidine base loading to 12.0 equiv with **Ni-1** then balanced both metrics, delivering 54% yield and 94% e.s. (entry 6), establishing the optimal protocol for the unprotected six-membered ring system. Not included in this table are the myriad other parameters evaluated, including solvents, bases, sulfonyl group identity (*42*), concentrations, temperature, and ligand architecture (see tables S1 to S11 for an extensive list). Applying these conditions to the analogous five-membered pyrrolidine substrate ($n = 0$) yielded only 3% of the coupling product but with a very high 88% e.s. (entry 7). This promising result suggested that the reaction could be improved based on what was achievable on the piperidine scaffold. To avoid a lengthy optimization campaign using a standard one-variable-at-a-time approach, we systemically investigated reaction conditions of the pyrrolidine scaffold with full-factorial high-throughput experimentation (HTE). This approach allowed us to rapidly screen the full reaction parameter space (Ni catalyst, solvent, base, and hydrazide), which demonstrated a complex interplay between these variables and highlighted the importance of a protecting group on the free pyrrolidine (see supplementary materials). Thus, HTE screening of ~1000 conditions guided subsequent refinements: Switching to **Ni-2** with a Ts group improved yield to 45% but dropped e.s. to 39% (entry 8), whereas Cbz (41% yield, 51% e.s.; entry 9), Boc (27% yield, 57% e.s.; entry 10), and Alloc (21% yield, 61% e.s.; entry 11) offered incremental gains in enantiospecificity at the expense of yield. The *para*-methoxyphenyl (PMP) protecting group with **Ni-2** achieved 28% yield and 89% e.s. (entry 12), but e.s. decreased to 79% with **Ni-1** (19% yield; entry 13); ultimately, **Ni-3** with PMP provided the best compromise for the five-membered system at 74% yield and 85% e.s. (entry 14), highlighting the nuanced interplay of ligand, protecting group, and ring size in achieving robust stereoretention in synthetically useful yield. A final round of optimization was conducted to see whether the scope of RRCC would permit the coupling of secondary alkyl iodides using hydrazide **17** and pyranyliodide **18**. Under optimized conditions (entry 14) applied to this reaction (entry 15), the yield of adduct **19** was good (74%), but the e.s. was modest (66%). A further round of catalyst screening led to substantial improvement with **Ni-1** delivering 71% isolated yield with 86% e.s. (entry 16), and, optimally, enlisting **Ni-2** delivered high yield of **19** (84%) while retaining 86% e.s. [93.0:7.0 enantiomeric ratio (e.r.); entry 17]. The ability to couple two transient secondary radicals in the absence of directing groups or chiral ligands is a notable strategic development for the retrosynthetic analysis of such systems.

With optimized conditions established for both piperidine ($n = 1$) and pyrrolidine ($n = 0$) scaffolds, the substrate scope of this enantiospecific RRCC (Fig. 3) demonstrated substantial breadth and functional group compatibility, enabling the modular assembly of diverse enantioenriched C(sp^3)–C(sp^3) linkages with consistently good yields (typically 40 to 90%) and excellent enantiospecificity (generally 80 to 96%). For piperidine-based sulfonylhydrazides, the reaction accommodates a wide array of alkyl iodides bearing ethers (**24** and **25**), acetal (**26**), heterocycles (**27** and **28**), trifluoromethyl group (**29**), terminal olefin (**30**), silyl-protected alcohol (**31**), and even sensitive motifs such as coumarin derivatives from hymecromone (**33**) and phthalimide (**34**, absolute configuration verified by x-ray crystallography of the corresponding *N*-tosylate **34-Ts**), with elevated temperatures (45°C) occasionally used

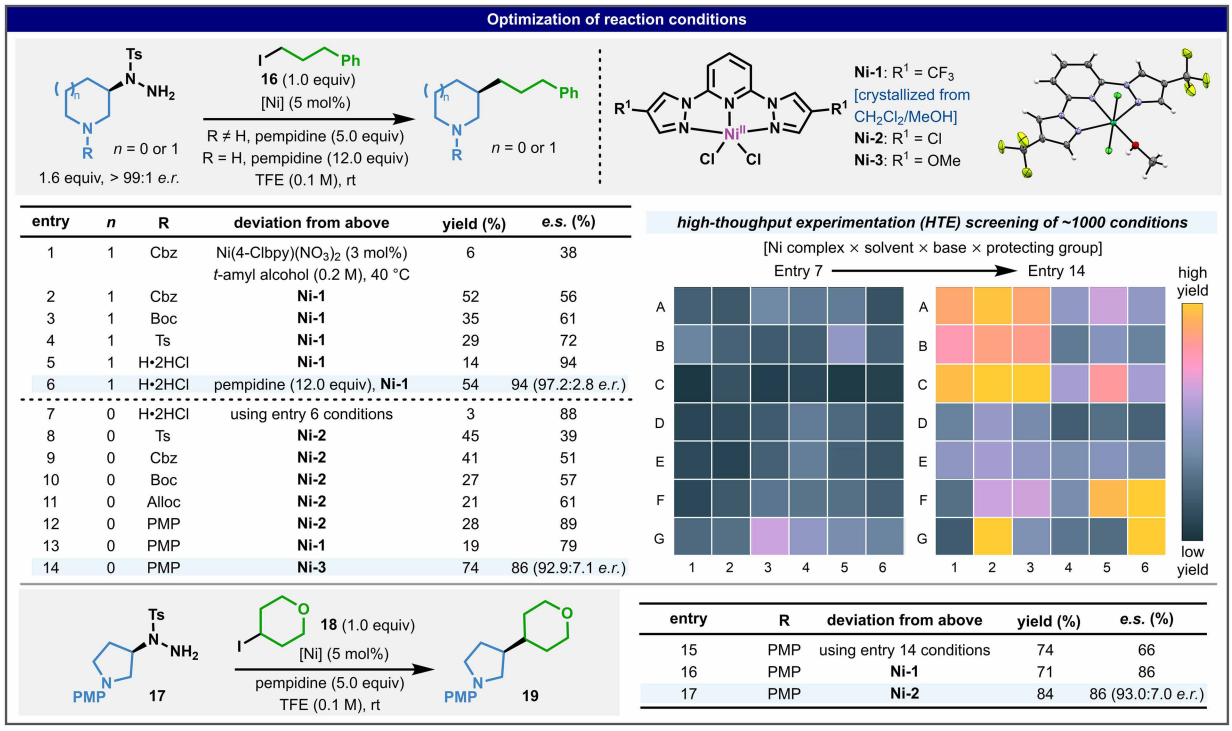

entry	n	R	deviation from above	yield (%)	e.s. (%)
1	1	Cbz	Ni(4-Clbpy)$(NO_3)_2$ (3 mol%) *t*-amyl alcohol (0.2 M), 40 °C	6	38
2	1	Cbz	**Ni-1**	52	56
3	1	Boc	**Ni-1**	35	61
4	1	Ts	**Ni-1**	29	72
5	1	H•2HCl	**Ni-1**	14	94
6	1	H•2HCl	pempidine (12.0 equiv), **Ni-1**	54	94 (97.2:2.8 *e.r.*)
7	0	H•2HCl	using entry 6 conditions	3	88
8	0	Ts	**Ni-2**	45	39
9	0	Cbz	**Ni-2**	41	51
10	0	Boc	**Ni-2**	27	57
11	0	Alloc	**Ni-2**	21	61
12	0	PMP	**Ni-2**	28	89
13	0	PMP	**Ni-1**	19	79
14	0	PMP	**Ni-3**	74	86 (92.9:7.1 *e.r.*)

entry	R	deviation from above	yield (%)	e.s. (%)
15	PMP	using entry 14 conditions	74	66
16	PMP	**Ni-1**	71	86
17	PMP	**Ni-2**	84	86 (93.0:7.0 *e.r.*)

Fig. 2. Reaction development and optimization of stereoretentive RRCC, including the use of HTE screening of conditions. bpy, 2,2'-bipyridine; Cbz, benzyloxycarbonyl; Ts, *p*-toluenesulfonyl; Alloc, allyloxycarbonyl; rt, room temperature.

for optimal reactivity. The coupling of an alkyl iodide bearing an aryl bromide is particularly compelling because only the desired product **32** was observed with no competitive arylation (51% yield, 93% e.s.). Notably, the use of TFE as solvent prevents undesired *N*-alkylation of the free amine in the piperidine core, which allows direct coupling without protecting groups in many cases. Secondary alkyl iodides could also be used when using *N*-PMP–protected piperidine derived hydrazide **21** to afford cyclopentenyl, cyclohexanone, and indanyl coupled derivatives **35**, **36**, and **37**. In these cases, the optimized conditions for the coupling of secondary halides with PMP-protected pyrrolidinyl sulfonylhydrazide **17** were used (Fig. 2, entry 17).

Extending to pyrrolidine scaffolds, the method maintains robustness with similarly diverse alkyl iodides, including those with free or silyl-protected alcohol (**39** and **41**), benzamides (**40**), and ketals [**43**, 90.0:10.0 diastereomeric ratio (d.r.), and **55**], and *gem*-difluoride (**56**), as well as spirocycles (**50** and **51**), cyclic systems (**52** and **57**), pyran (**53**), and Cbz-protected piperidine (**54**). Even challenging substrates such as isoxepac-derived iodides (**58**) or benzyl bromides (as alternatives to iodides; **44**, **45**, and **46**) proceeded smoothly. Compatibility with unsaturation (prenyl and propargyl linked adducts **47** and **48** derived from prenyl and propargyl bromide, respectively) as well as sensitive azetidine (**42** and **50**) and oxetane (**49**) ring systems stands as a testament to the high chemoselectivity of RRCC. Across both ring systems, the average yield is 61% with 87% average e.s., which reflects practical utility, whereas the high e.s. values preserve substrate stereoconfiguration with fidelity, even on the gram scale (vide infra).

Such enantioenriched alkyl-alkyl architectures, particularly those featuring saturated heterocycles ubiquitous in pharmaceuticals, such as piperidines and pyrrolidines, are notoriously difficult to access using traditional methods owing to inherent mechanistic barriers in $C(sp^3)$–$C(sp^3)$ cross-coupling, including β-hydride elimination, sluggish oxidative addition, and poor stereocontrol in polar or radical pathways. Conventional polar cross-couplings often require activated partners (e.g., benzylic or α-heteroatom stabilized centers) or chiral ligands tailored to specific substrates, which limits generality and necessitates lengthy resolutions or auxiliary-guided syntheses that inflate step counts. Enantioconvergent radical approaches, although promising, typically demand exogenous redox agents, stabilized radicals, or dual-catalyst systems and struggle to couple transient alkyl radical fragments without racemization on picosecond timescales. By contrast, this RRCC leverages achiral Ni catalysts and bench-stable precursors for direct, redox-neutral coupling, bypassing these issues and streamlining access to complex chiral motifs that would otherwise require multistep sequences involving olefin reductions, alkylations, or fragmentations. The chiral sulfonylhydrazide starting materials are accessible from the chiral pool (thousands of chiral amines and alcohols are commercial) or can be prepared by easily scalable industrial processes (transaminase, lipase, or asymmetric reduction).

Synthetic utility

With a set of optimized conditions in hand, the strategic application of stereoretentive RRCC was evaluated in the context of a medicinally relevant structure and a natural product (Fig. 4A). The brominated piperidine **1** mentioned in Fig. 1 was used en route to NPY-Y1 receptor antagonists and served as a linchpin intermediate for downstream S_N2 chemistry (*40*). A logical route using polar-bond analysis comprising seven steps was previously reported, involving a single strategic C–C bond forming step (Horner–Wadsworth–Emmons reaction on nicotinaldehyde) along with redox manipulations, chiral resolution, and functional group interconversions. A more direct path to **1** would necessitate the union of hydrazide **20** with commercial 3-iodo-1-bromopropane **59**. Given the known enhanced rate of XAT of an alkyl iodide versus an alkyl bromide (*46*), we reasoned that RRCC would proceed with position control at the desired C–I bond. Notably, RRCC union of **20** and **59** proceeded smoothly to deliver **1** in 60% isolated yield (95% e.s., 97.4:2.6 e.r.). The convergent simplicity of such a route can open opportunities in a medicinal chemistry program to alter the chain length or substitution on the alkyl iodide fragment to enable rapid access to

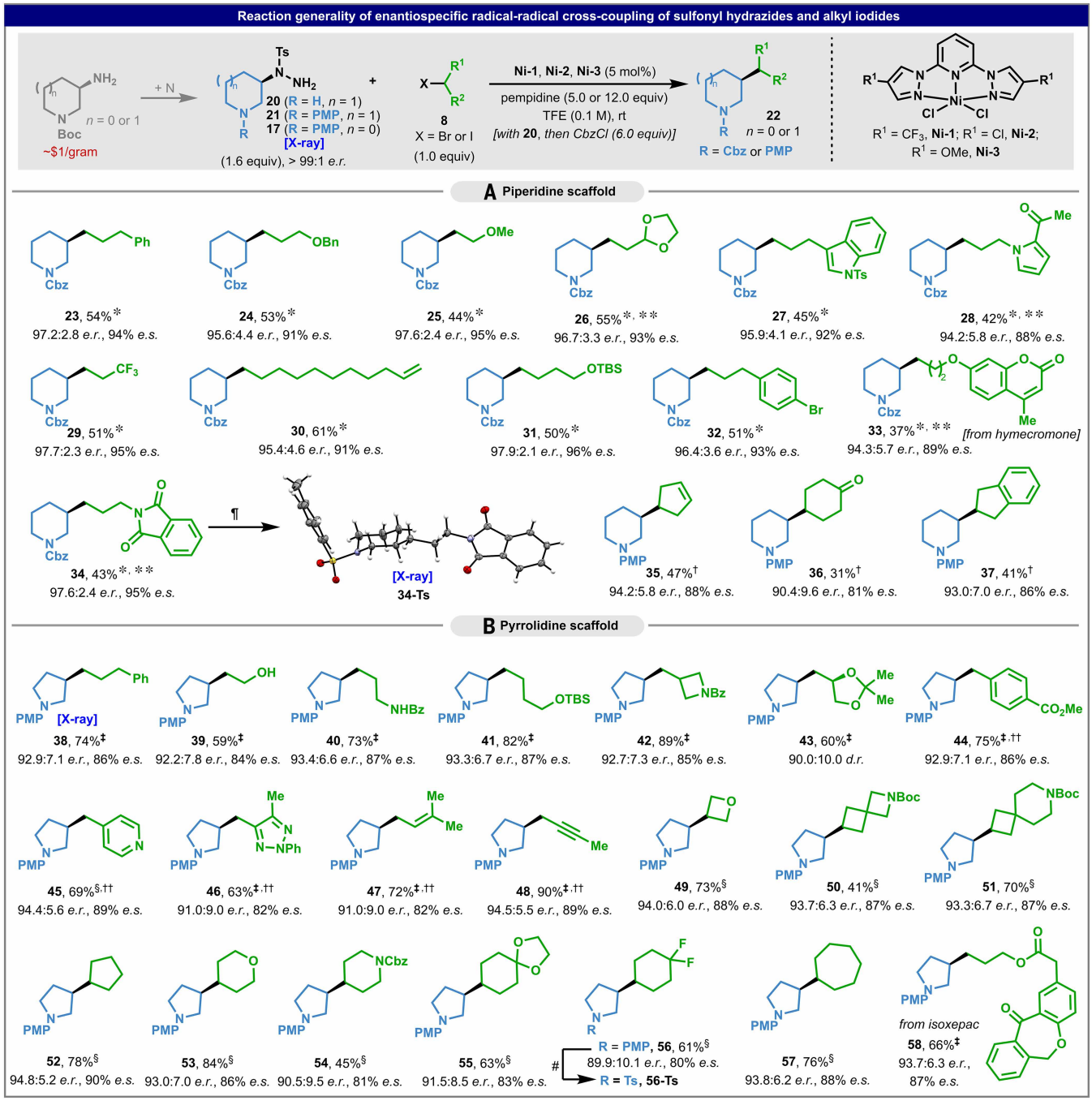

Fig. 3. Generality and scope of stereoretentive RRCC. *Using hydrazide **20**, **Ni-1**, 12.0 equiv pempidine. †Using hydrazide **21** and **Ni-2**. ‡Using hydrazide **17** and **Ni-3**. §Using hydrazide **17** and **Ni-2**. ¶Reaction condition: BCl_3 (6.0 equiv), DCM, 0°C; then TsCl (1.2 equiv), Et_3N (3.0 equiv), tetrahydrofuran (THF):H_2O (1:1), 0°C to rt, 67%. #Reaction condition: CAN (3.0 equiv), MeOH:MeCN:H_2O (1:1:1), 0°C to rt, then TsCl (2.0 equiv), $NaHCO_3$ (5.0 equiv), DCM, 0°C to rt, 73%. **Reaction run at 45°C. ††Alkyl bromide was used instead of alkyl iodide. CAN, ammonium cerium(IV) nitrate.

diversity. Next, (*S*,*S*)-stenusine (**62**), a natural product previously prepared four different ways (supplementary materials, section 7.2), was targeted. The most efficient of the known syntheses is depicted and required chiral-auxiliary assisted diastereoselective hydrogenation of a pyridine in a six-step route; 8 days of extended reaction time were needed for both auxiliary installation and high-pressure hydrogenation (*47*). By contrast, RRCC of **20** (2.0 equiv) and commercial chiral iodide **60** delivered **61** in 42% isolated yield (10.6:1 d.r.) after in situ Boc protection (to ease purification). Subsequent one-pot deprotection and reductive amination delivered **62**, highlighting a substantial advantage in the directness and speed of this approach. As with stereoretentive arylation via RCC, alkylation through RRCC can enable useful levels of diastereoselectivity (Fig. 4B). For instance, hydrazide **63**, derived from 3-amino-proline, was subjected to RRCC with alkyl iodide **64** to deliver adduct **65** in 43% yield as a 3.6:1 mixture favoring the cis-product. As expected, conventional RRCC (under electrochemical control) furnished a 1:1.2 mixture of isomers favoring the trans-product in low yield. Although that electrochemical result could certainly be optimized to improve reactivity, the diastereoselectivity would likely remain low. Finally, stereoretentive RRCC is scalable (Fig. 4C), as evidenced

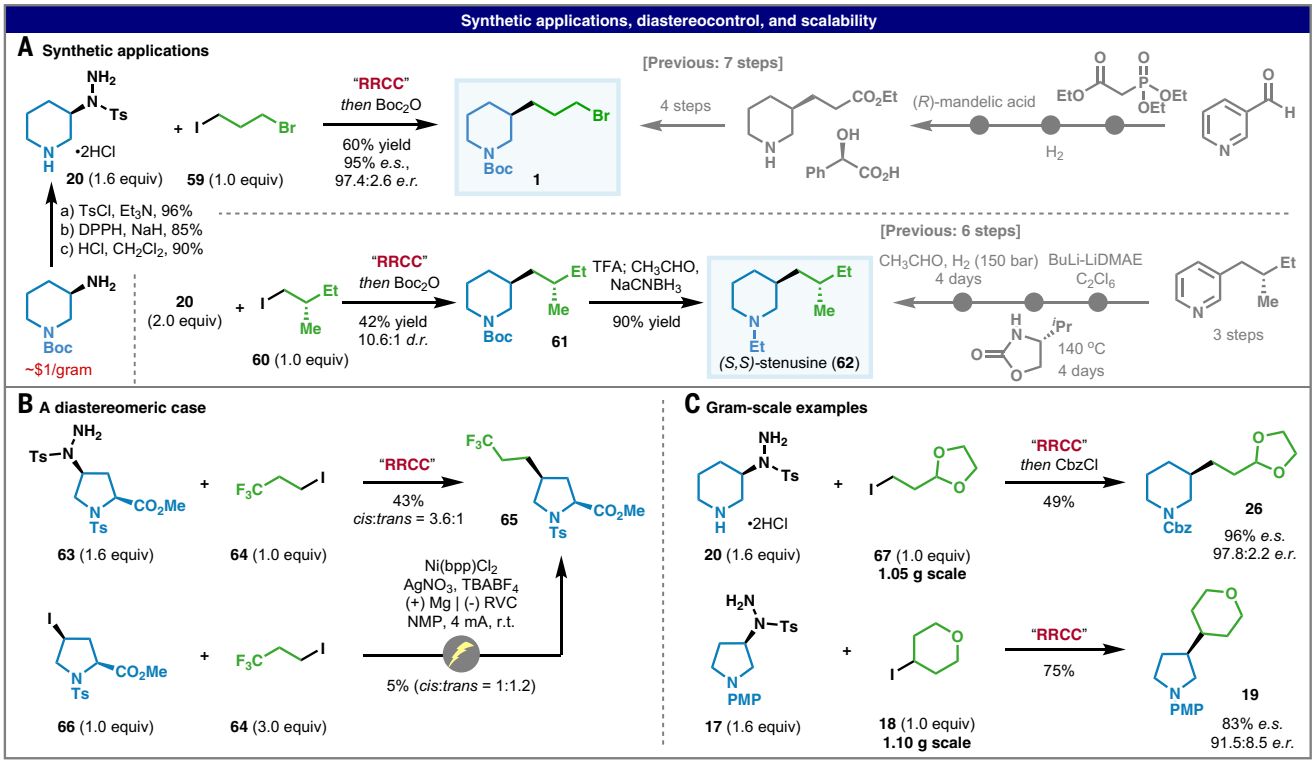

Fig. 4. Synthetic applications, diastereocontrol, and scalability. (**A**) Applications of stereoretentive RRCC to approach drug intermediates and natural products. (**B**) Diastereomeric studies demonstrate the different reaction outcomes between sulfonylhydrazides and canonical electrochemical coupling using alkyl iodide. (**C**) Scaled-up RRCC examples forming acetal and pyran-containing products in good yields and enantiospecificities.

by the gram-scale preparation of piperidine **26** (49% isolated yield, 97.8:2.2 e.r.) and pyrrolidine **19** (75% isolated yield, 91.5:8.5 e.r.).

Mechanistic investigation

To elucidate the mechanistic pathway underlying this enantiospecific RRCC, a suite of experimental and computational investigations was undertaken, revealing a radical-radical process supported by a critical caged radical rebound step that preserves stereochemical fidelity without a chiral catalyst. First, cyclopropyl radical clock experiments confirmed the radical nature of the transformation (Fig. 5A). Using hydrazide **68** and cyclopropylmethyl iodide **69**, rearranged product **70** was observed (55% yield), confirming the intermediacy of an alkyl radical derived from the halide. Next, the iodide and hydrazide functionalities were swapped, and alkyl iodide **72** was treated with cyclopropylmethyl hydrazide **73**. Rearranged product **70** was observed (34% yield) as the major species, confirming the presence of an alkyl radical intermediate from the hydrazide partner as well. Notably, a small amount of direct coupling product (**71**, 4% yield, 1:8 ratio with **70**) was also observed. As irreversible cyclopropylcarbinyl radical rearrangement occurs in nanoseconds [rate constant (k) = 2×10^8 s^{-1}, half-life ($t_{1/2}$) = 3.5 ns at 45°C] (*48*), and thus formation of this direct product indicates that radical capture by Ni occurs on the picosecond-to-nanosecond timescale and suggests a caged radical-rebound process (*49*–*51*). Consistent with this finding, the reaction of slower 6-*exo*-trig hydrazide radical clock (k = 3×10^5 s^{-1} at 30°C) (*52*) delivered exclusively the direct coupling product in 48% yield (supplementary materials), in sharp contrast to traditional free radical capture by Ni(II) complexes, which gives mostly the rearranged product after 6-*exo* cyclization (*52*). Additional radical clock investigations are shown in the supplementary materials, section 9, and also support caged radical-rebound at Ni.

Computational analyses complemented these findings and are summarized in Fig. 5B. Using model hydrazide **74** (which when treated with alkyl iodide **16** gives chiral product **23** in 94% e.s.), the reaction coordinate was investigated by dispersion-corrected density functional theory (DFT) quantum chemical calculations performed in the ORCA 6 software package (*53*). Association of **74** to the Ni catalyst gives **75** [total spin (S) = 1, Gibbs free energy (ΔG) = 4.7 kcal mol^{-1}], followed by deprotonation of the hydrazide by tertiary amine base to triplet **76** and loss of sulfinate-amine salt (ΔG = 8.6 kcal mol^{-1}). A second deprotonation event gives Z-bound diazene intermediate **77** through a modestly downhill process (S = 1, ΔG = 7.5 kcal mol^{-1}). Rotation about the chiral C–N bond affords intermediate **78**, with isoenergetic singlet (S = 0, ΔG = 28.5 kcal mol^{-1}) and triplet geometries (S = 1, ΔG = 28.2 kcal mol^{-1}). This intermediate appears stabilized by an agostic-type interaction between the Ni and the C–H bond adjacent to the diazene (Ni–C, distance of 2.23 Å) and exhibits considerable spin density accumulation at nickel, the chiral carbon, and both nitrogen atoms of the diazene (supplementary materials), indicative of an open-shell species primed for homolytic cleavage. In fact, traversing a modest barrier of $\Delta G^{\ddagger}$ = 7.9 kcal mol^{-1} gives open-shell singlet transition state $\mathbf{TS}_A$ (ΔG = 36.1 kcal mol^{-1}). Löwdin analysis finds atoms Ni, N, N, and C carrying spin densities of 0.758, −0.228, −0.093, and −0.372, respectively, illustrating the synchronous formation of a d^9 Ni(I) complex alongside an alkyl radical and molecular dinitrogen.

The alkyl radical fragment has two possible fates: It may exit the cage to give racemic free radical **79** and Ni(I) complex **80** (S = 1/2, ΔG = −7.2 kcal mol^{-1}), or it may remain in the cage as **83** and undergo rapid rebound to Ni, affording stereoretentive Ni–alkyl complex **82** (S = 0, ΔG = −27.2 kcal mol^{-1}). Closer analysis of this bifurcation is given in Fig. 5C, where energies (red data) and spin density (blue and orange data) of the caged Ni–radical pair are given as a function of Ni–C bond

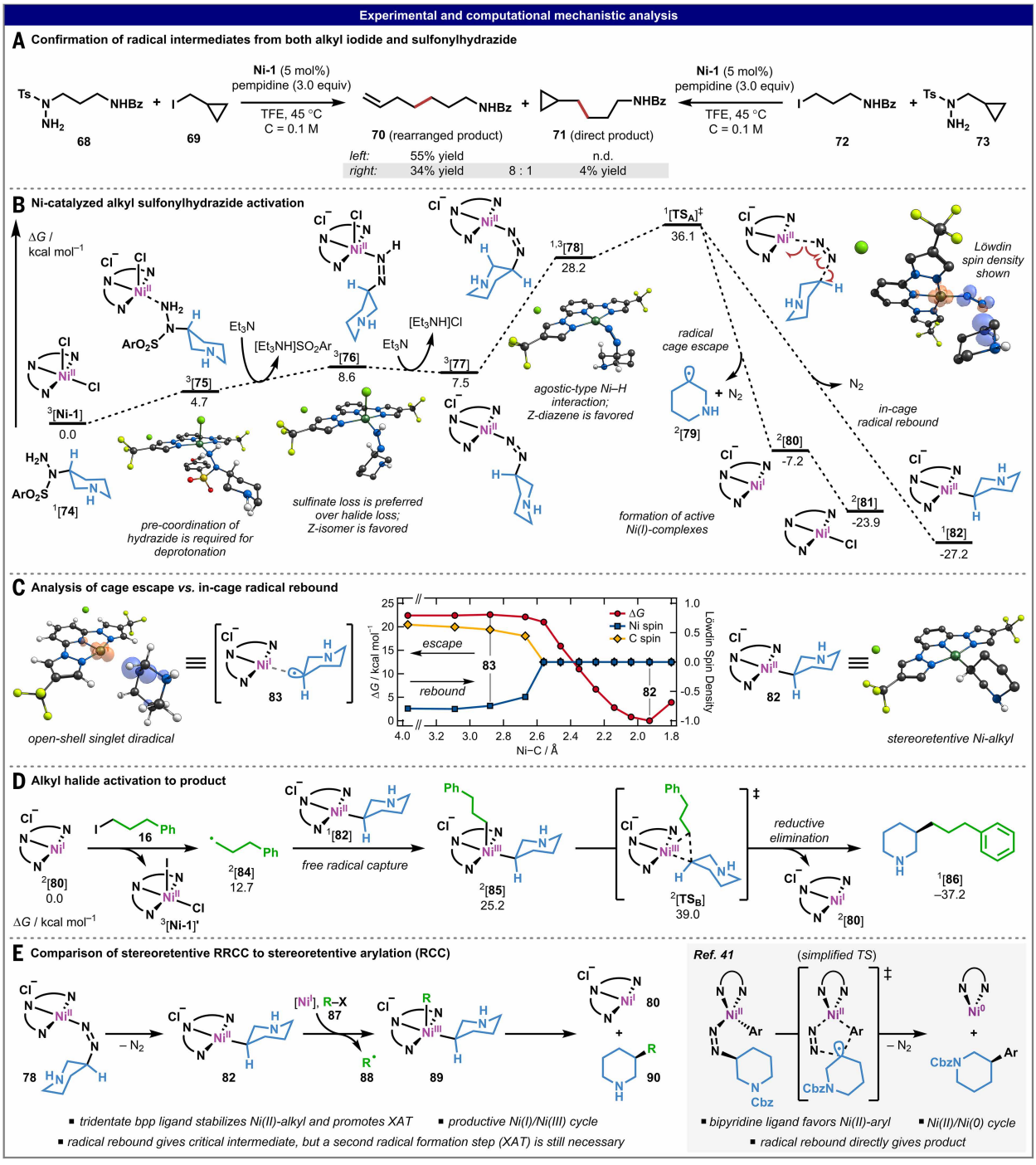

Fig. 5. Proposed reaction pathways and associated mechanistic analysis. (**A**) Radical clock experiments confirm a dual-radical pathway. (**B**) DFT analysis of Ni-catalyzed alkyl sulfolyl hydrazide activation. (**C**) Investigation of cage-escape versus rebound pathways using relaxed potential energy surface scan and associated Löwdin spin density analysis along the Ni–C bond coordinate. (**D**) Alkyl halide activation, free radical capture, and product formation. (**E**) Comparison of the mechanism found in this work with stereoretentive arylation. Optimized geometries found at the (U)TPSSh-D3(BJ) def2-TZVPP(Ni), def2-TZVP, ma-def2-TZVP (Cl, I) CPCM(TFE) level of theory; electronic energies computed with (U)B3LYP-D3B(J) def2-QZVPP(Ni), def2-TZVPP, ma-def2-TZVPP (Cl, I) CPCM(TFE). See the supplementary materials for more details. Computed free energies are given in kilocalories per mole.

distance. When the atomic distance between the atoms is >3.0 Å, cage escape is likely to occur. However, at smaller Ni–C distances, radical rebound is purely associative and strongly favorable; no barrier was found between **83** and **82**. DFT analysis therefore suggests that the stereoretentive pathway is dependent on in-cage radical rebound, a process that is sensitive to temperature, solvent, and the general reaction conditions—an observation that is in good agreement with the optimization and screening results presented in Fig. 2 and tables S1 and S7 to S11.

Formation of the enantiopure product is possible through Ni-catalyzed activation of the alkyl halide (Fig. 5D). DFT suggests that Ni(I) species **80** engages in formal XAT with alkyl iodide **16** to give free alkyl

radical **84** and return the starting Ni catalyst (with halogen exchanged, [**Ni-1**]′; $\Delta G = 12.7$ kcal mol^{-1}). Intermediate **82** captures this radical to yield Ni(III) complex **85** ($S = 1/2$, $\Delta G = 25.2$ kcal mol^{-1}), which surmounts a barrier of $\Delta G^{\ddagger} = 13.8$ kcal mol^{-1} to reach doublet $\mathbf{TS}_B$. Reductive elimination from $\mathbf{TS}_B$ is thermodynamically favorable, returns Ni(I) species **80**, and gives the chiral product **86** ($\Delta G = -37.2$ kcal mol^{-1}). Critically, the product-forming pathway is a closed Ni(I)-Ni(III) cycle that also returns the **Ni-1** precatalyst; only a small fraction of active Ni(I) must be generated for product formation, thereby enabling simultaneous high yield and enantiospecificity under ideal conditions. This mechanistic postulate allows for free radical capture of secondary radicals (derived from 2°-iodides), particularly given the low steric encumberance about Ni species **82** owing to the planar ligand used.

Key differences between stereoretentive RRCC and our previous work on stereoretentive arylation (*41*) arise when considering the formation and stabilization of the critical Ni(II)–alkyl intermediate **82** (Fig. 5E). Although N_2 extrusion and radical rebound directly afforded the enantiopure arylation product, stereoretentive alkylation requires **82** to persist long enough to capture the free radical from the alkyl halide. Tridentate ligands such as those used in this work have been demonstrated to aid in the formation of such Ni–alkyl species, whereas the bidentate ligands used previously lend toward stable Ni(II)–aryl complexes (*43*). Moreover, RCC was found by DFT to proceed through a Ni(II)-Ni(0) cycle, whereas the present work begins with Ni(II), which subsequently enters a Ni(I)-Ni(III) productive cycle. Therefore, although this mechanism is inspired by our previous work on stereoretentive arylation through radical-polar coupling, it now extends to alkyl-alkyl bond formation. Enantiopure alkyl sulfonylhydrazides function as a transient radical precursor (via diazenes) that recombine within a Ni complex cage to preserve substrate chirality and release enantioenriched products through Ni(I)-mediated radical activation of alkyl halides and subsequent reductive elimination. The substantial driving force to initialize this RRCC process is redox-neutral nitrogen extrusion, providing nearly 30 kcal mol^{-1} of energy before the C(sp^3)–C(sp^3) bond is even formed. Additional supporting computational and mechanistic analysis, including the analysis of alternate pathways, intermediates, and transition states, are presented in the supplementary materials, section 10.4; the full proposed mechanistic cycle is given in the supplementary materials, section 10.7.

Conclusions

Decades of physical organic chemistry studies on transient carbon-based radicals have demonstrated that instantaneous racemization occurs upon generation from enantiopure precursors. Thus, the community has focused exclusively on enantioconvergent strategies for radical cross-coupling. Stereoretentive RCC arylation demonstrated that capture of a transient radical is possible through a diazene-linked transition state to an aryl-metal complex. This study takes this finding to the next level by coupling two transient radicals with stereochemical control. This work opens the door to a distinct way of approaching the retrosynthetic analysis of complex stereopure organic molecules.

REFERENCES AND NOTES

1. E. Geist, A. Kirschning, T. Schmidt, *Nat. Prod. Rep.* **31**, 441–448 (2014).
2. H. Yamamoto, E. M. Carreira, Eds., *Comprehensive Chirality*, vol. 1 (Elsevier, 2012).
3. F. Lovering, J. Bikker, C. Humblet, *J. Med. Chem.* **52**, 6752–6756 (2009).
4. F. Lovering, *MedChemComm* **4**, 515–519 (2013).
5. F. Diederich, P. J. Stang, Eds., *Metal-Catalyzed Cross-Coupling Reactions* (Wiley, 2008).
6. M. J. Gibian, R. C. Corley, *Chem. Rev.* **73**, 441–464 (1973).
7. A. de Meijere, S. Bräse, M. Oestreich, Eds., *Metal-Catalyzed Cross-Coupling Reactions and More* (Wiley, 2013).
8. J. Choi, G. C. Fu, *Science* **356**, eaaf7230 (2017).
9. J. M. Smith, S. J. Harwood, P. S. Baran, *Acc. Chem. Res.* **51**, 1807–1817 (2018).
10. M. Yan, J. C. Lo, J. T. Edwards, P. S. Baran, *J. Am. Chem. Soc.* **138**, 12692–12714 (2016).
11. G. Laudadio, M. D. Palkowitz, T. El-Hayek Ewing, P. S. Baran, *ACS Med. Chem. Lett.* **13**, 1413–1420 (2022).
12. Y. Gong, J. Hu, C. Qiu, H. Gong, *Acc. Chem. Res.* **57**, 1149–1162 (2024).
13. S. B. Beil, T. Q. Chen, N. E. Intermaggio, D. W. C. MacMillan, *Acc. Chem. Res.* **55**, 3481–3494 (2022).
14. A. Y. Chan *et al.*, *Chem. Rev.* **122**, 1485–1542 (2022).
15. A. Cook, S. G. Newman, *Chem. Rev.* **124**, 6078–6144 (2024).
16. B. Zhang *et al.*, *Nature* **623**, 745–751 (2023).
17. B. Zhang *et al.*, *Nature* **606**, 313–318 (2022).
18. Y. Hioki *et al.*, *Science* **380**, 81–87 (2023).
19. S. Al Zubaydi *et al.*, *Nature* **634**, 585–591 (2024).
20. Z. Huang, M. E. Akana, K. M. Sanders, D. J. Weix, *Science* **385**, 1331–1337 (2024).
21. W. Liu, M. N. Lavagnino, C. A. Gould, J. Alcázar, D. W. C. MacMillan, *Science* **374**, 1258–1263 (2021).
22. R. Chen *et al.*, *Science* **383**, 1350–1357 (2024).
23. X. Yu, T. Yang, S. Wang, H. Xu, H. Gong, *Org. Lett.* **13**, 2138–2141 (2011).
24. K. Komeyama, T. Michiyuki, I. Osaka, *ACS Catal.* **9**, 9285–9291 (2019).
25. W. Zhang *et al.*, *Nature* **604**, 292–297 (2022).
26. P. Li *et al.*, *Nat. Catal.* **7**, 412–421 (2024).
27. E. L. Lucas, E. R. Jarvo, *Nat. Rev. Chem.* **1**, 0065 (2017).
28. W.-T. Zhao, J.-X. Zhang, B.-H. Chen, W. Shu, *Nat. Commun.* **14**, 2938 (2023).
29. L.-L. Zhang, L.-J. Li, N. Wang, H. Yu, Z.-P. Yang, *J. Am. Chem. Soc.* **147**, 33097–33107 (2025).
30. H. Fu *et al.*, *Nature* **610**, 302–307 (2022).
31. D. Uraguchi, N. Kinoshita, T. Kizu, T. Ooi, *J. Am. Chem. Soc.* **137**, 13768–13771 (2015).
32. W.-T. Zhao, W. Shu, *Sci. Adv.* **9**, eadg9898 (2023).
33. C. Wang *et al.*, *Angew. Chem. Int. Ed.* **55**, 685–688 (2016).
34. J. Ma *et al.*, *J. Am. Chem. Soc.* **139**, 17245–17248 (2017).
35. S. Byun *et al.*, *Angew. Chem. Int. Ed.* **62**, e202312829 (2023).
36. Y. Xu *et al.*, *Nature* **625**, 74–78 (2024).
37. V. Tseliou *et al.*, *Nature* **634**, 848–854 (2024).
38. J. Li *et al.*, *Nat. Catal.* **7**, 889–899 (2024).
39. T. Li, Z. Xu, Y. Huang, W. Zu, H. Huo, *J. Am. Chem. Soc.* **147**, 10999–11009 (2025).
40. H. Zarrinmayeh *et al.*, *J. Med. Chem.* **41**, 2709–2719 (1998).
41. J. Sun *et al.*, *Nature* **642**, 85–91 (2025).
42. D. A. Cagan *et al.*, *J. Am. Chem. Soc.* **148**, 677–691 (2026).
43. T. J. Anderson, G. D. Jones, D. A. Vicic, *J. Am. Chem. Soc.* **126**, 8100–8101 (2004).
44. G. A. Dawson, Q. Lin, M. C. Neary, T. Diao, *J. Am. Chem. Soc.* **145**, 20551–20561 (2023).
45. L. E. Ehehalt *et al.*, *Chem. Rev.* **124**, 13397–13569 (2024).
46. Q. Lin, Y. Fu, P. Liu, T. Diao, *J. Am. Chem. Soc.* **143**, 14196–14206 (2021).
47. T. Müller, K. Dettner, K. Seifert, *Eur. J. Org. Chem.* **2011**, 6032–6038 (2011).
48. M. Newcomb, in *Encyclopedia of Radicals in Chemistry, Biology and Materials*, C. Chatgilialoglu, A. Studer, Eds. (Wiley, 2012).
49. F. Ogliaro *et al.*, *J. Am. Chem. Soc.* **122**, 8977–8989 (2000).
50. L. Liu, W. Lee, J. Zhou, S. Bandyopadhyay, O. Gutierrez, *Tetrahedron* **75**, 129–136 (2019).
51. Z. Qiu, C. N. Neumann, *ACS Org. Inorg. Au* **4**, 1–25 (2024).
52. Q. Lin, E. H. Spielvogel, T. Diao, *Chem* **9**, 1295–1308 (2023).
53. F. Neese, *WIREs Comput. Mol. Sci.* **12**, e1606 (2022).

ACKNOWLEDGMENTS

We thank G. J. Kroon and L. Pasternack (Scripps Research) for nuclear magnetic resonance (NMR) spectroscopic assistance, M. Gembicky (UCSD) for x-ray analysis, and J. Lee and Q. N. Wong (Scripps Automated Synthesis Facility). We also thank J. He for helpful discussion and A. Pollatos for proofreading. **Funding:** This project is financially supported by the National Institutes of Health (GM-118176; to P.S.B.). D.A.C. acknowledges support through the National Science Foundation MPS-Ascending postdoctoral fellowship (NSF 2500003). The computations presented in this work were conducted in the Garibaldi High Performance Computing (HPC) cluster, a facility supported by Scripps Research, La Jolla. **Author contributions:** Y.W., J.S., Y.K., and P.S.B. conceptualized the study. Y.W., J.S., Y.L., D.A.C., O.T.R., X.Z., J.T., L.M., and M.R.C. conducted the experimental investigation. Y.W., J.S., Y.L., D.A.C., O.T.R., X.Z., J.T., L.M., J.E.S., B.J.O., Y.K., and P.S.B. performed the data analysis. D.A.C. designed and performed the DFT calculations. D.A.C., J. T., and B.J.O. designed and performed the HTE screen. Y.W., J.S., Y.L., D.A.C., O.T.R., X.Z., J.T., Y.K., and P.S.B. wrote the paper. Y.K. and P.S.B. helped with the fund acquisition. P.S.B. conceived and supervised the project. **Competing interests:** The authors declare no competing interests. **Data, code, and materials availability:** Crystallographic data are available free of charge from the Cambridge Crystallographic Data Centre under CCDC 2515803 (compound **Ni-1**), 2518181 (compound **17**), 2504806 (compound **34-Ts**), and 2515804 (compound **38**). All other characterization data and details for the synthesis of all reported compounds are available in the supplementary materials.

SUPPLEMENTARY MATERIALS

science.org/doi/10.1126/science.aef6981
Supplementary Text; Figs. S1 to S28; Tables S1 to S30; NMR Spectra; References (*54*–*93*)
Submitted 21 January 2026; accepted 14 April 2026
10.1126/science.aef6981

Stereoretentive radical-based alkyl-alkyl cross-coupling

Yu Wang, Jiawei Sun, Yin Li, David A. Cagan, Oliver T. Ring, Xin Zeng, Jet Tsien, Luca Massaro, Jillian E. Smith, Brandon J. Orzolek, Michael R. Collins, Yu Kawamata, and Phil S. Baran

Science **392** (6802), . DOI: 10.1126/science.aef6981

Editor's summary

Chemical bond-forming reactions fall into two categories: ionic mechanisms with electron pair intermediates and radical mechanisms with unpaired electrons. Generally, the radical intermediates have fluctuating configurations and so tend to deliver two mirror-image products. Wang *et al*. present a protocol for coupling two alkyl radicals in which the nickel catalyst captures one of them so rapidly that it retains the configuration of its precursor. Constructing a library of homochiral sulfonylhydrazide precursors thereby enables versatile radical coupling to enantioenriched products without chiral catalysts. —Jake S. Yeston